Influence of local atomic configuration in AlGdN phosphor thin films on deep ultra-violet luminescence intensity

Kitayama, Shinya ; Yoshitomi, Hiroaki ; Iwahashi, Shinya ; Nakamura, Junya ; Kita, Takashi ; Chigi, Yoshitaka ; Nishimoto, Tetsuro ; Tanaka…

(Citation)
Journal of Applied Physics,110(9):093108-093108

(Issue Date)
2011-11-01

(Resource Type)
journal article

(Version)
Version of Record

(URL)
https://hdl.handle.net/20.500.14094/90001624

Influence of local atomic configuration in AlGdN phosphor thin films on deep ultra-violet luminescence intensity

Shinya Kitayama,[1] Hiroaki Yoshitomi,[1] Shinya Iwahashi,[1] Junya Nakamura,[1] Takashi Kita,[1,a)]
Yoshitaka Chigi,[2] Tetsuro Nishimoto,[2] Hiroyuki Tanaka,[2] Mikihiro Kobayashi,[2]
Tsuguo Ishihara,[3] and Hirokazu Izumi[3]
[1]*Department of Electrical and Electronic Engineering, Graduate School of Engineering, Kobe University, 1-1 Rokkodai, Nada, Kobe 657-8501, Japan*
[2]*YUMEX INC., Itoda 400, Yumesaki, Himeji, Hyogo, Japan*
[3]*Hyogo Prefectural Inst. of Tech., 3-1-12Yukihira, Suma, Kobe, Japan*

(Received 4 April 2011; accepted 6 October 2011; published online 9 November 2011)

We investigated the narrowband ultraviolet emission properties of $Al_{0.94}Gd_{0.06}N$ phosphor thin films pumped by an electron beam. An extremely narrow luminescence line, which was less than 1 nm from the intra-orbital *f-f* transition in Gd^{3+} ions, was confirmed at 318 nm. The corresponding emission efficiency was improved by decreasing the growth temperature. The extended X-ray absorption fine structure analysis of the local atomic structure revealed that a low-temperature growth led to the formation of a uniform atomic configuration around Gd, which was found to play a key role in improving the luminescence intensity of the films. © *2011 American Institute of Physics*. [doi:10.1063/1.3658845]

I. INTRODUCTION

Ultraviolet (UV)-light sources are widely used in various applications, including photolithography, polymerization, curing, sterilization, and medical treatments. However, current UV-light sources such as excimer and mercury lamps have serious issues related to low emission efficiency and the presence of harmful constituents and many unnecessary emission lines. Thus, the development of a novel mercury-free UV-light source has become crucial. Recently, nitride-semiconductor-based UV-light-emitting diodes (UV-LEDs) that can emit at various wavelengths have been developed.[1–4] The emission wavelength of UV-LEDs can be controlled by changing the alloy compositions of AlGaN and InAlGaN multiple-quantum-well structures. However, the output power is lowered significantly when the emission wavelength is shortened because of the resulting difficulty in controlling the electronic conductivity. As a result, the use of an electron-beam pumping technique for UV-light emission is attracting strong interest.[5] These devices are based on the band-edge emission of nitride semiconductor heterostructures and enable the achievement of strong emission intensities. However, the spectrum line width determined by the carrier population near the band edge is relatively broad, that is, it is generally more than 10 nm. Such a broad line width is not suitable for photolithography and medical treatment applications[6] because they require the use of narrowband UVB (Ultraviolet B; wavelength from 280 to 315 nm). Even by using currently available single-chip UV-LEDs, it is not easy to achieve a spectral power density of 1 mW/nm in the deep-UV region.

Instead of using band-edge emission, we focused on the use of narrowband emissions from the intra-orbital *f-f* transition of a rare-earth ion. The optical transition of the intra-4*f* orbital of a Gd trivalent ion results in a luminescence line at approximately 320 nm with a very narrow line width of less than 1 nm.[7–14] The line width is extremely narrow because of the electromagnetic shield effect, and therefore, the corresponding emission wavelength is temperature insensitive. To avoid the absorption of the emission from Gd^{3+} ions, the host material must have a wide bandgap of more than 4 eV. AlN, which is a III–V compound semiconductor, is suitable for this requirement because it has a bandgap of approximately 6 eV.

In our previous work, we reported the properties of narrowband UV emission from $Al_{1-x}Gd_xN$ phosphor thin films pumped by an electron beam. $Al_{1-x}Gd_xN$ thin films were grown by a reactive radio-frequency magnetron sputtering method in an ultra-high vacuum system with a base pressure of less than 5.0×10^{-6} Pa, and the emission efficiency was found to depend on various conditions such as the growth temperature and Gd concentration. In particular, the emission intensity was improved by decreasing the growth temperature.[12] However, a low-temperature growth degrades the long-range ordering of the wurtzite atomic structure. This result seems to contradict with the improved emission intensity observed in the case of $Al_{1-x}Gd_xN$ grown at a low growth temperature. To understand this contradiction, we studied the influence of the local atomic structure around Gd^{3+} ions using extended X-ray absorption fine structure (EXAFS) analysis in this study and discussed the relationship between the local atomic configuration and luminescence intensity.

II. GROWTH OF AlGdN PHOSPHOR THIN FILMS AND CHARACTERIZATIONS

$Al_{1-x}Gd_xN$ phosphor films were grown using a reactive radio-frequency magnetron sputtering technique.[11–14] A deposition chamber equipped with three targets was separated

a)Author to whom correspondence should be addressed. Electronic mail: kita@eedept.kobe-u.ac.jp.

from a substrate-introduction chamber. The back pressure of the growth chamber was less than approximately 5×10^{-6} Pa. We used a 6N mixed gas of argon and nitrogen for the reactive growth, and the partial pressure ratio was even. The total sputtering pressure was 5 Pa. 4N Al and 3N Gd were used as the metal targets. When growing $Al_{1-x}Gd_xN$, we set Gd metal tips on the Al target. The GdN mole fraction x of 6% was controlled by changing the number of tips. The phosphor film with the mole fraction GdN of 6% exhibits the concentration quenching in luminescence.[14] In this work, we investigated the high Gd-concentration phosphor films to understand clearly the quenching mechanism caused by the growth temperature. We grew 300-nm-thick $Al_{0.94}Gd_{0.06}N$ films on fused silica substrates at 100, 200, 300, 400, and 500 °C. Furthermore, in Sec. VI, we investigated the effects of a buffer layer of AlN inserted before growing the $Al_{0.94}Gd_{0.06}N$ layer on the luminescence intensity. The buffer layer thickness was varied in the range of 0–1200 nm, and a 1000-nm-thick $Al_{0.94}Gd_{0.06}N$ film was grown on it. The growth temperature for both the buffer and phosphor layers was 200 °C.

X-ray diffraction (XRD) measurements were carried out at room temperature using Cu-K_α line. By changing the configuration of the goniometer, the out-of-plane and in-plane θ-2θ diffraction spectra were measured. EXAFS measurements in a fluorescence mode at the room temperature were performed using a beam line of a synchrotron radiation facility with a high-energy storage ring of 8 GeV (SPring-8).[15] The Gd-L_3 edge of $Al_{0.94}Gd_{0.06}N$ was detected and analyzed the radial structure function around Gd ions. By analyzing the line shape of the analyzed radial structure function with using *ab initio* self-consistent multiple scattering calculations, we evaluated the Debye-Waller factor representing the inhomogeneous lattice distortion.

Properties of the UV-light emission from $Al_{0.94}Gd_{0.06}N$ phosphor layer were investigated by measuring cathode luminescence (CL) at room temperature. The CL spectrum was measured using a single monochromator with the spectral resolution of 1.02 nm and detected by a Si charge-coupled device (CCD). The CL measurements were carried out at the acceleration voltage of 3.0 kV and the injected electron current of 0.2 mA in vacuum of 2.0×10^{-4} Pa. According to the depth profile of the absorbed power density of injected electrons calculated by the Monte Carlo method, the penetration depth of the accelerated electrons into the film was estimated to be approximately 120 nm which is smaller than the $Al_{0.94}Gd_{0.06}N$ film thickness.

III. CRYSTALLOGRAPHIC PROPERTIES OF AlGdN PHOSPHOR THIN FILMS

We measured the XRD spectra of $Al_{0.94}Gd_{0.06}N$ films grown at different temperatures. 300-nm-thick $Al_{0.94}Gd_{0.06}N$ films used here were grown on fused silica substrates. The results are shown in Fig. 1. The magnified (0002) diffraction signal is shown in Fig. 1(b). The spectral line width is almost independent of the growth temperature. With an increase in temperature, the diffraction peak shifts toward the high-angle side because of the thermal expansion mismatch between the film and the substrate. All the films exhibit a c-axis preferential orientation. High preferential orientation was achieved at high growth temperatures. It was found that c-axis-oriented polycrystalline $Al_{0.94}Gd_{0.06}N$ was obtained even at 100 °C. Figure 2 shows the typical XRD spectra measured for the (1) out-of- and (2) in-plane directions for AlN grown at 200 °C. The out-of-plane XRD spectrum shows a c-axis orientation. On the other hand, the in-plane XRD spectrum shows diffraction lines arising from different planes. This result indicates that the in-plane orientation is random. Thus, the AlN film deposited on the fused silica substrate is concluded to be a c-axis-oriented polycrystal.

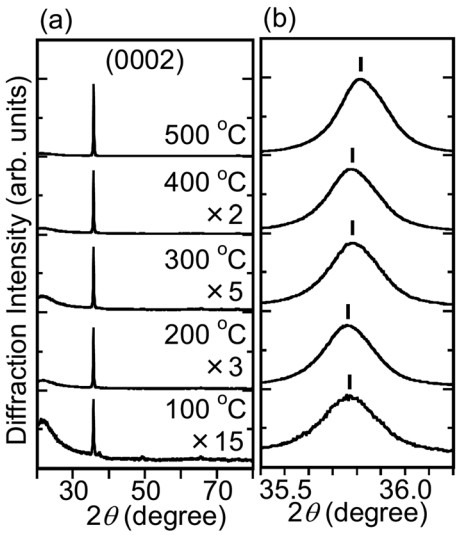

FIG. 1. The XRD spectra of $Al_{0.94}Gd_{0.06}N$ films grown at different temperatures are shown in (a). The magnified signals of the (0002) diffraction are shown in (b).

IV. LOCAL ATOMIC STRUCTURE AROUND Gd IONS

We carried out EXAFS measurements for the Gd-L_3 edge of $Al_{0.94}Gd_{0.06}N$ and analyzed the radial structure function around Gd ions. 300-nm-thick $Al_{0.94}Gd_{0.06}N$ films were directly grown on fused silica substrates. Figure 3 shows the

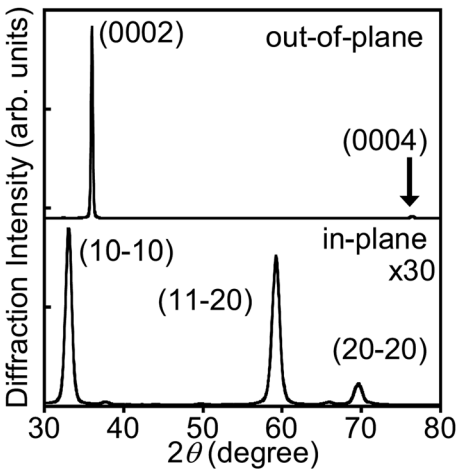

FIG. 2. XRD spectra of an AlN thin film measured for out- and in-plane directions.

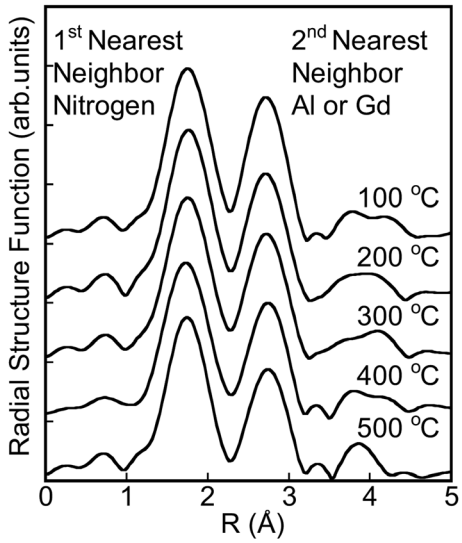

FIG. 3. Radial structure function of $Al_{0.94}Gd_{0.06}N$ thin films grown at different temperatures.

results; the peak at 1.8 Å corresponds to the 1st nearest neighbor site of nitrogen and the next peak at 2.8 Å is attributed to the next-nearest-neighbor III-group sites of Al or Gd. We could not specifically confirm whether GdN clusters with the rocksalt structure were formed in $Al_{0.94}Gd_{0.06}N$.[12,13] This implied that Gd atoms correctly occupied the Al sites. The signal intensity of the 2nd nearest neighbor was found to be highly sensitive to the growth temperature as compared to that of the 1st nearest neighbor. By analyzing the line shape of the observed radial structure function, we evaluated the Debye–Waller factors representing the inhomogeneity of the lattice distortion around Gd. This result is summarized in Fig. 4. With the decrease in the growth temperature, the Debye–Waller factors of both the 1st and the 2nd nearest neighbor sites decreased. In particular, the change in the factor of the 2nd nearest neighbor site, which was related to the ordering of the group III atoms, was drastic. This indicated that a low growth temperature can suppress the inhomogeneous distribution of Gd atoms. Generally, when we prepare a mixture of two or more components with different chemical compositions and physical properties, the mixture can separate into distinct phases. The crystal symmetry of GdN is rocksalt and the lattice constant is large.[16] Therefore, it is easy for the local Gd concentration to increase. When the growth temperature is increased, it is considered that the inhomogeneous formation of Gd-rich regions results in a distributed local lattice distortion.

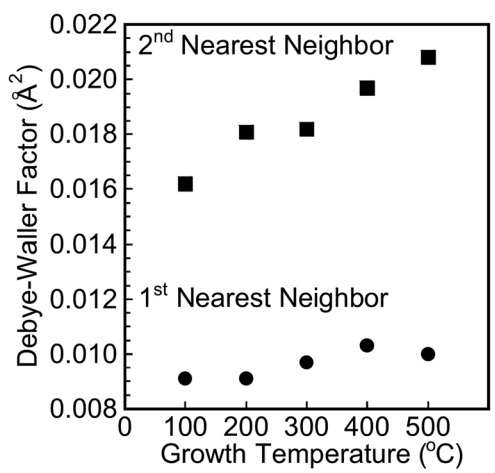

FIG. 4. Debye–Waller factor of the 1st and 2nd nearest neighbor sites as a function of growth temperature.

V. LUMINESCENCE INTENSITY OF AlGdN PHOSPHOR THIN FILMS DEPENDING ON GROWTH TEMPERATURE

Figure 5 shows a typical CL spectrum obtained from a 300-nm-thick $Al_{0.94}Gd_{0.06}N$ thin film grown at 200 °C on a fused silica substrate. The spectrum shows a strong, sharp peak at 318 nm, which corresponds to the transition from the lowest excited states $^6P_{7/2}$ to the ground state $^8S_{7/2}$. The line width was approximately 1 nm. This peak was confirmed to consist of several sharp lines caused by the Stark splitting.[14] A CL peak appeared at 312 nm can be attributed to the transition from the second lowest excited states $^6P_{5/2}$ to the ground state $^8S_{7/2}$. The inset of Fig. 5 shows a growth temperature dependence of the CL intensity. The CL intensity is dramatically enhanced by lowering the growth temperature; the CL intensity of the film grown at 100 °C is approximately one order stronger than that of the film grown at 500 °C. It is well known that there are two excitation mechanisms: direct impact ionization and the indirect excitation done by energy transfer from electron-hole pairs generated in the host crystal into Gd centers. Generally, the intra-orbital electron transition is insensitive to the environment. So, the direct excitation efficiency is considered to be hardly influenced by the atomic configurations. Actually, the slight change in the radial structure function for the second nearest neighbor hardly influences to the CL peak wavelength and the decay time. Therefore, the drastic growth temperature dependence of the CL intensity observed indicates that the indirect excitation process is dominant. On the other hand, as mentioned in Sec. III, high preferential orientation was observed at high growth temperatures. The CL intensity, however, becomes small with the growth temperature. It is a puzzle that the low degree of the long-range ordering of the atomic structure at

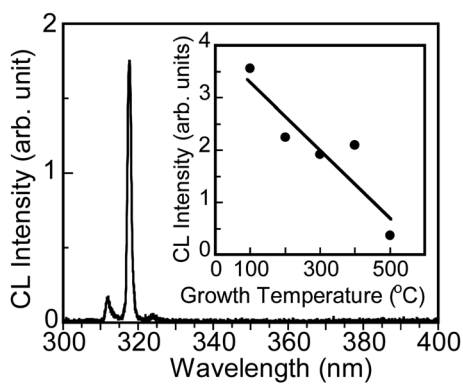

FIG. 5. Typical cathode luminescence spectrum obtained at 3 kV and 0.2 mA. The inset shows the growth temperature dependence of CL intensity.

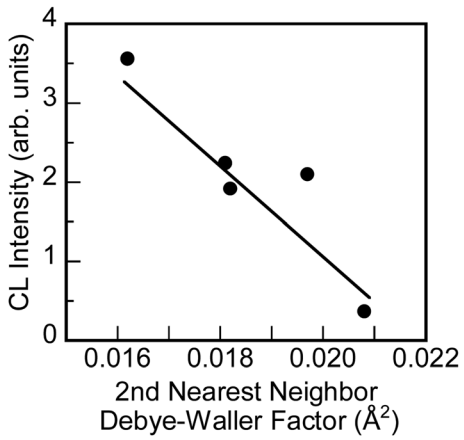

FIG. 6. CL intensity as a function of the 2nd nearest neighbor's Debye–Waller factor.

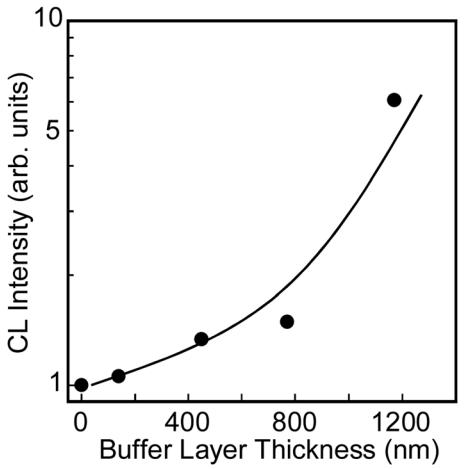

FIG. 7. AlN-buffer layer thickness dependence of CL intensity.

low growth temperatures causes an efficient indirect excitation. To make clear the origin of the CL enhancement observed in the phosphor thin film grown at the low temperatures, we compared the CL intensity with the EXAFS data. Figure 6 shows a relationship between the CL intensity and the Debye–Waller factor of the 2nd nearest neighbor site. The luminescence intensity is improved by reducing the Debye–Waller factor. As mentioned above, a small value of the Debye–Waller factor indicates a relatively uniform atomic configuration around Gd atoms in the AlN matrix. In other words, the relatively large mean distance among Gd atoms inhibits the quenching of the luminescence intensity.

VI. IMPROVED LUMINESCENCE INTENSITY BY INTRODUCING THICK BUFFER LAYER

Finally, we discuss the effects of the AlN buffer layer on the luminescence efficiency. To enhance the emission efficiency, we need to suppress the composition aggregation of Gd. However, a low growth temperature degrades the long-range ordering of the wurtzite structure. To improve the long-range ordering even at a low growth temperature, we introduced a thick AlN buffer layer. The buffer layer thickness was varied in the range of 0–1200 nm, and a 1000-nm-thick $Al_{0.94}Gd_{0.06}N$ film was grown on it. The growth temperature for both the buffer and phosphor layers was 200 °C. Figure 7 shows the buffer-layer-thickness dependence of the CL intensity. With an increase in the buffer layer thickness, the CL intensity was found to enhance remarkably. The (0002)-X-ray diffraction intensity normalized by the film thickness increased with the buffer-layer thickness. This indicates the improvement in the wurtzite ordering. In the case of the indirect excitation mechanism, the CL intensity is enhanced by suppressing the non-radiative recombination process via crystal defects formed in the host material. Introduction of the buffer layer apparently improved the long-range ordering of the wurtzite structure, which is considered to reduce crystal defects, and resultantly, the CL intensity becomes strong.

VII. SUMMARY

We have studied the influence of the local atomic structure around the Gd^{3+} ions in $Al_{0.94}Gd_{0.06}N$ phosphor thin films on the deep-UV luminescence intensity using XRD, EXAFS, and CL measurements. The narrowband luminescence line from Gd^{3+} ions was observed at 318 nm. The luminescence intensity was enhanced by decreasing the growth temperature, which in turn caused the formation of a uniform atomic configuration around Gd. To improve wurtzite ordering even at a low growth temperature of less than 200 °C, we introduced a thick AlN buffer layer and found that the luminescence intensity increased as a result.

[1]H. Hirayama, S. Fujikawa, N. Noguchi, J. Norimatsu, T. Takano, K, Tsubaki, and N. Kamata, Phys. Status Solidi A **206**, 1176 (2009).
[2]A. Bhattacharyya, T. D. Moustakas, L. Zhou, D. J. Smith, and W. Hug, Appl. Phys. Lett. **94**, 181907 (2009).
[3]H. Hirayama, Y. Tsukada, T. Maeda, and N. Kamata, Appl. Phys. Express **3**, 031002 (2010).
[4]A. Fujioka, T. Misaki, T. Murayama, Y. Narukawa, and T. Mukai, Appl. Phys. Express **3**, 041001 (2010).
[5]T. Oto, R. G. Banal, K. Kataoka, M. Funato, and Y. Kawakami, Nat. Photonics **4**, 767 (2010).
[6]J. A. Parrish and K. F. Jaenicke, J. Invest. Dermatol. **76**, 359 (1981).
[7]U. Vetter, J. Zenneck, and H. Hofsäss, Appl. Phys. Lett. **83**, 2145 (2003).
[8]B. J. Gruber, U. Vetter, H. Hofsäss, B. Zandi, and M. F. Reid, Phys. Rev. B **69**, 195202 (2004).
[9]M. J. Zavada, N. Nepal, Y. J. Lin, X. H. Jiang, E. Brown, U. Hömmerich, J. Hite, T. G. Thaler, C. R. Abernathy, and S. J. Pearton, Appl. Phys. Lett. **89**, 152107 (2006).
[10]M. Maqbool, I. Ahmad, H. H. Richardson, and E. M. Kordesch, Appl. Phys. Lett. **91**, 193511 (2007).
[11]T. Kita, S. Kitayama, M. Kawamura, O. Wada, Y. Chigi, Y. Kasai, T. Nishimoto, H. Tanaka, and M. Kobayashi, Appl. Phys. Lett. **93**, 211901 (2008).
[12]S. Kitayama, T. Kita, M. Kawamura, O. Wada, Y. Chigi, Y. Kasai, T. Nishimoto, H. Tanaka, and M. Kobayashi, IOP Conf. Ser.: Mater. Sci. Eng. **1**, 012001 (2009).
[13]T. Kita, S. Kitayama, H. Yoshitomi, T. Ishihara, H. Izumi, Y. Chigi, Y. Kasai, T. Nishimoto, H. Tanaka, and M. Kobayashi, J. Ceram. Proc. Res. **12**(Special 1), 73 (2011).
[14]T. Kita, S. Kitayama, T. Ishihara, H. Izumi, Y. Chigi, T. Nishimoto, H. Tanaka, and M. Kobayashi, Proc. 2011 Spring Meeting (in press).
[15]See http://www.spring8.or.jp/en/ for information about 8GeV synchrotron radiation facility.
[16]H. Yoshitomi, S. Kitayama, T. Kita, and O. Wada, Phys. Rev. B **83**, 155202 (2011).